Journal of Photochemistry and Photobiology A: Chemistry 274 (2014) 57–63

Contents lists available at ScienceDirect

Journal of Photochemistry and Photobiology A: Chemistry

journal homepage: www.elsevier.com/locate/jphotochem

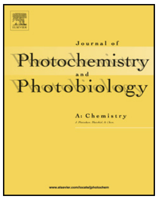

Synthesis and photophysical studies of triazine-linked porphyrin–perylene bisimide dyad with long-lived perylene triplet state

Xueqin Zhou[a], Dongzhi Liu[a], Tianyang Wang[a], Xiaoxia Hu[a], Jianfeng Guo[a], Krishanthi C. Weerasinghe[b], Lichang Wang[b], Wei Li[a,*]

[a] School of Chemical Engineering and Technology, Tianjin University, Tianjin 300072, PR China
[b] Department of Chemistry and Biochemistry, Southern Illinois University, Carbondale, IL 62901, USA

ARTICLE INFO

Article history:
Received 28 June 2013
Received in revised form
26 September 2013
Accepted 30 September 2013
Available online 21 October 2013

Keywords:
Electron transfer
Energy transfer
Porphyrin
Perylene
Donor–acceptor system

ABSTRACT

Porphyrin–perylene bisimide dyad containing a triazine group as the linker was synthesized and characterized. The absorption spectra reveal that there is no appreciable interaction between the ground-state porphyrin and ground-state perylene. The fluorescence spectra illustrate that photoinduced energy transfer takes place from the excited perylene to ground-state porphyrin moiety when excited at 491 nm, while enhanced photoinduced electron transfer occurs from the porphyrin singlets to ground-state perylene moiety in the case of excitation at 423 nm. The kinetic analysis indicates that a long-lived perylene triplet state (146 μs) forms via triplet–triplet energy transfer from the porphyrin to perylene moiety, showing potential applications in the photodynamic therapy. These photochemical events are explained with an energy-level diagram.

1. Introduction

In the natural photosynthesis, sun-lights are absorbed by photofunctional chromophores and are funneled to realize the biopolymer conversion and energy storage [1]. The essential processes are the efficient photo-induced energy and electron transfer among various singlets, triplet excited states and ground states in the photosynthetic reaction center, which result in the formation of the charge-separated excited states [1–3]. Studies of these processes have led to the development of photocatalysts and solar energy conversion systems such as organic donor–acceptor solar cells and dye sensitized solar cells [2,3]. Relative triplet states are capable to react with oxygen to produce highly reactive oxygen species, which can destroy the tumor cells, springing up the photodynamic therapy of cancers and other diseases [4]. Among various photofunctional chromophores, porphyrin-based donor–acceptor arrays have received much interest owing to structural similarity of porphyrins to the natural light-harvesting chromophores in the photosynthetic reaction centers [2]. The efficiency of dye-sensitized solar cells fabricated with asymmetric porphyrin derivatives has been reported as high as 12.3% by Grätzel and co-authors [5]. Porphyrin derivatives have also been found applications as the photosentisizers for the photodynamic therapy of cancers, cardiovascular and ophthalmic diseases by effective accumulation within tumor tissues [6], excitation with relative long wavelength light (650–800 nm) and effective generation of singlet oxygen via their long-lived triplet states (several to about hundred microseconds) [7,8]. Anthraquinones [9], fullerenes [10], oxadiazoles [11] and perylenes [12] are common electron acceptors in porphyrin donor–acceptor systems due to their low LUMO and small reorganizational energies. Specially, the intense absorption bands of perylene derivatives are between porphyrin's Soret band and Q bands, thus perylenes can enhance the absorption efficiency of the sunlight and is thought to be a better acceptor candidate [13,14].

Substituted perylenes were linked assembly or covalently to the porphyrin directly [15,16] or indirectly through imide [17], ether [18], or alkyne [19] group. It has been shown that the linker affects the distance, angle, relative orientation and coupling energies between the donor and the acceptor, which significantly influence the photoinduced electron transfer and charge recombination processes [20]. Previously we have investigated the optical

---

* Corresponding author at: School of Chemical Engineering, Tianjin University, Tianjin 300072, PR China. Tel.: +86 22 27400911; fax: +86 22 27892283.
E-mail addresses: zhouxueqin@tju.eudu.cn (X. Zhou), liwei2008@tju.edu.cn (W. Li).

1010-6030/$ – see front matter © 2013 Elsevier B.V. All rights reserved.
http://dx.doi.org/10.1016/j.jphotochem.2013.09.018

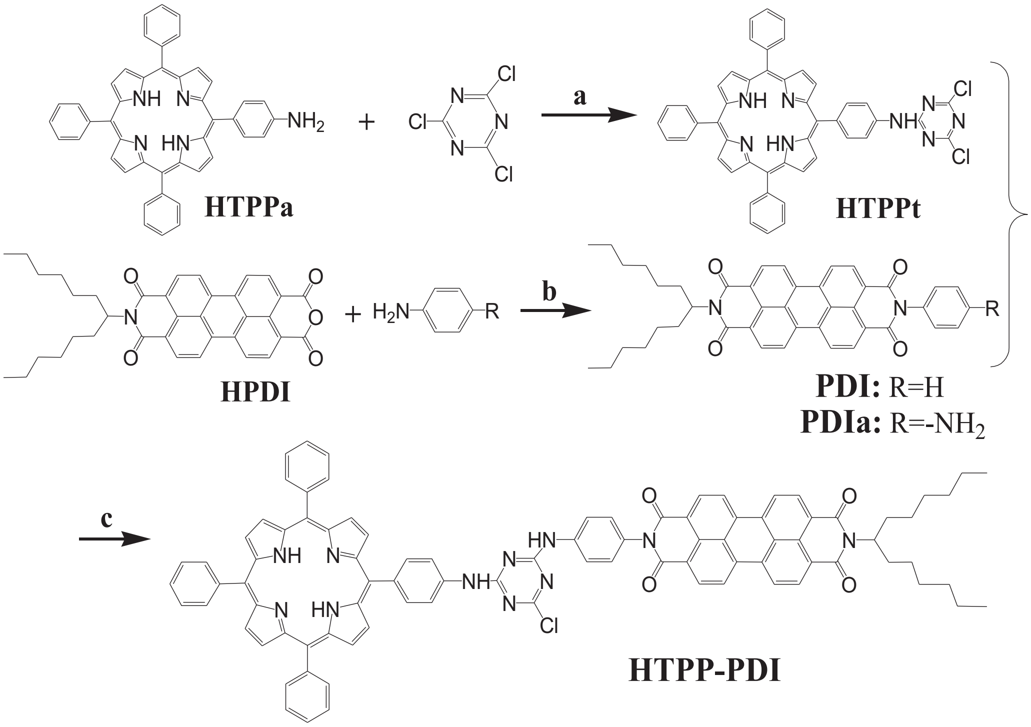

Scheme 1. Synthesis scheme of dyad **HTPP–PDI**. (a) TEA, 0 °C-rt, 1 h; (b) imidazole, 130 °C, 5 h; (c) N_2, NaH, 80 °C, 4 h.

properties of porphyrin–anthraquinone and porphyrin–oxadiazole dyads bridged by various groups, among which the triazine linker was found favoring intramolecular photoinduced electron transfer process from the excited donor to the acceptor moiety while effectively blocking the charge recombination process [21,22]. In this paper the triazine group was employed to link the porphyrin and perylene bisimide (Scheme 1) to explore the efficiency of the triazine linker in other donor–acceptor arrays. Studies of the intramolecular/intermolecular energy and electron transfer of synthesized dyad **HTPP–PDI** are discussed in detail. Long-lived perylene triplet state was found with a lifetime as long as 146 μs, showing potential applications in the photodynamic therapy.

2. Experimental

2.1. General

5,10,15,20-Tetraphenylporphyrin (**HTPP**), 5-(4-aminophenyl)-10,15,20-triphenylporphyrin (**HTPPa**) and N-(1-hexylheptyl) perylene-3,4,9,10-tetracarboxyl-3,4-anhydride-9,10-imide (**HPDI**) were prepared as reported [21,23,24]. All other reagents and solvents were in reagent grade and further purified by the standard methods if necessary. Infrared spectra were recorded on a NICOLET380. ^{1}H NMR spectra were obtained on a Varian INOVA-500MHZ superconducting spectrometer. FAB and ESI mass spectra were obtained on an Autoflex Tof/Tof III mass spectrometer and microOTOF-Q II mass spectrometer, respectively. Absorption spectra were taken on a Nicolet Evolution 300 UV–visible spectrometer. Fluorescence spectra were recorded on a Varian ECLIPSE fluorospectrophotometer. Electrochemical properties were measured using a BAS 100 W electrochemical analyzer and performed in a three-electrode cell. A glassy carbon electrode was used as working electrode, Ag/$AgNO_3$ electrode as reference electrode and platinum as auxiliary electrode. The scan rate was 100 mV/s. Dichloromethane with 0.05 mol/L tetrabutylammonium hexafluorophosphate ($TBAPF_6$) was employed as the medium for all the cyclic voltammetric experiments. Nanosecond transient absorption spectra were carried out by LP920 laser-flash photolysis apparatus with, a Nd:YAG laser (532 nm) as the exciting source and a pulsed xenon flash lamp as monitor light. All solutions were purged using nitrogen gas prior to the transient absorption spectral determination and electrochemical measurement.

2.2. Synthesis

2.2.1. N-(1-Hexylheptyl)-N′-phenyl perylene-3,4,9,10-tetracarboxylbisimide (*PDI*)

In a 100 mL round-bottom flask, **HPDI** (100 mg, 0.174 mmol), phenylamine (162 mg, 1.74 mmol) and imidazole (2.00 g, 29.3 mmol) were added to 35 mL toluene. The solution was refluxed for 8 h. The reaction mixture was cooled to room temperature upon which 25 mL water was added. The aqueous fraction was separated, and then re-extracted three times with dichloromethane. All organic fractions were combined, dried over $MgSO_4$ and then stripped of solvent. Purification of the product by column chromatography over silica gel (CH_2Cl_2) gave **PDI** as red solid (63.2 mg, 56.3%). MALDI-TOF-MS (*m/z*): 649.682 $[M+H]^+$.

2.2.2. N-(1-Hexylheptyl)-N′-(4-amino)phenyl perylene-3,4,9,10-tetracarboxylbisimide (*PDIa*)

In a 100 mL round-bottom flask, **HPDI** (900 mg, 1.53 mmol), 1,4-diaminobenzene (1.65 g, 15.3 mmol) and imidazole (20 g, 0.3 mol) were stirred 5 h at 130 °C under nitrogen. The reaction mixture was cooled to room temperature, and then dispersed into 200 mL ethanol. Afterwards 200 mL 2 M HCl was added to the mixture, followed by stirring overnight. The dark red precipitate was filtered and rinsed thoroughly with water, and dried at 80 °C to give 760 mg (74.9%) of red solid. FT-IR (cm^{-1}): 3432, 3378, 2953, 2925, 2855, 1698, 1657, 1594, 1507, 1406, 1360, 1250; ESI-MS (*m/z*): 664.3168 $(M+H)^+$.

Table 1
Half-wave redox potentials (V vs SCE), **HOMO** (eV) and **LUMO** for synthesized porphyrin and perylene compounds in dichloromethane.

Compound	$E_{1/2}^{-/2-}$	$E_{1/2}^{0/-}$	$E_{1/2}^{+/0}$	$E_{1/2}^{2+/+}$	**HOMO**	**LUMO**
HTPP	−1.69	−1.32	0.96	1.34	−5.70	−3.42
HTPPa	−1.70	−1.35	–	–	–	−3.39
HTPPt	−2.03	−1.45	1.01	1.42	−5.75	−3.29
PDI	−0.99	−0.69	1.71	–	−6.45	−4.05
PDIa	−0.93	−0.69	–	–	–	−4.05
HTPP–PDI	−0.92	−0.69	0.94	1.27	−5.68	−4.05

*2.2.3. 5-(4-(3,5-Dichloro triazine) aminophenyl)-10,15,20-triphenylporphyrin hydrochloride (**HTPPt**)*

HTPPa (25 mg, 0.04 mmol) dissolved in THF (1.0 mL) was added into solution of cyanuric chloride (7.3 mg, 0.04 mmol) and triethylamine (TEA) (4.8 mg, 0.048 mmol) in THF (2.0 mL) at 0 °C. After stirring at 0 °C for 10 min, the solution was warmed to and then kept at room temperature. After the reaction completed by monitoring with thin layer chromatography (TLC), the solvent was removed by rotary evaporation. The residue was purified by column chromatography on silica gel. A blue violet solid (29 mg) yielded (90.6%). ^{1}H NMR ($CDCl_3$, ppm), δ: 8.92–8.91 (d, J = 4.8 Hz, 2H, C_4H_5N β-H), 8.88–8.86 (d, J = 6.0 Hz, 6H, C_4H_5N β-H), 8.24–8.19 (m, 8H, $-C_6H_5$), 8.01–7.99 (d, J = 8.0 Hz, 2H, $-C_6H_5$), 7.79–7.74 (m, 10H, $-C_6H_5$, —NH·HCl), 7.45 (s, 1H, —NH), −2.72 (s, 2H, NH); ESI-MS (*m*/*z*): 814.4 $(M+HCl)^+$, 777.4 $(M+H)^+$.

*2.2.4. 5-{4-[3-Chloro-5-(N-(1-hexylheptyl)-N′-(4-amino)phenyl perylene-3,4,9,10-tetracarboxylbis-imide)triazine] aminophenyl}-10,15,20-triphenyl porphyrin (**HTPP–PDI**)*

To a suspension of **PDI** (60 mg, 0.09 mmol) in dry DMF (15 mL) was added NaH (2.1 mg, 0.09 mmol) at 0 °C. As the mixture reached room temperature, **HTPPt** was added. Then the mixture was heated to and kept stirring at 80 °C under nitrogen for 4 h. The solvent was removed under reduced pressure and the residue was purified by column chromatography on silica gel. Yield of product **HTPP–PDI** was 40 mg (33%). ^{1}H NMR ($CDCl_3$, ppm), δ: 8.89–8.56 (m, 12H), 8.19–7.47 (m, 23H), 7.25–7.27 (m, 4H), 5.14 (s, 1H), 2.20 (s, 4H), 1.97 (s, 4H), 1.59 (s, 4H), 1.27 (s, 8H), 0.86 (s, 6H), −3.53 (s, 2H, NH); MALDI-TOF-MS (*m*/*z*): 1404.409 $(M+H)^+$.

3. Results and discussion

3.1. Electrochemical properties

The electrochemical data for synthesized porphyrin and perylene derivatives are summarized in Table 1. **HTPP** shows two reversible oxidation waves (0.96 and 1.34 V vs SCE in CH_2Cl_2) and two reversible reduction waves (−1.32 and −1.69 V vs SCE in CH_2Cl_2). The first oxidation potential is in consistence with the reported data (0.99 V vs SCE in CH_2Cl_2) [25]. **HTPPa** only exhibits two reversible reduction waves due to the instability of amino group, which gives little effect on the reduction potentials of **HTPP**. However, 4,6-dichloro-1,3,5-triazineamine group in compound **HTPPt** can obviously increase the oxidation potentials and decrease the reduction potentials due to its electron withdrawing and steric effects. **PDI** shows one reversible oxidation wave (1.71 V vs SCE in CH_2Cl_2) and two reversible reduction waves (-0.99 and −0.69 V vs SCE in CH_2Cl_2). The first redox potentials, which were calculated as −1.14 and 1.26 V vs Fc/Fc^+, are consistent with the reported values of N,N′-dialkyl or diaryl perylene derivatives (at ca. −0.98 and 1.21 V vs Fc/Fc^+ in CH_2Cl_2) [26], indicating little effect of the N,N′ substituents on the redox potentials even in asymmetric perylene derivatives. This is due to the location of the **LUMO** (and **HOMO**) on the core [26], the orbital energies being modified by inductive effects of N,N′ substituents relayed via the imide nitrogen atoms. So it is reasonable that **PDIa** also shows similar reduction potentials.

When **HTPP** and **PDI** were linked by a triazine group, the redox potentials of the resulted dyad **HTPP–PDI** exhibit only a little change in comparison with porphyrin and perylene derivatives. As shown in Fig. 1, the dyad shows four reversible reduction waves (−1.71, −1.35, −0.92 and −0.69 V vs SCE in CH_2Cl_2), of which the first two reduction potentials agree with those of perylene derivatives and another two correspond to those of porphyrin derivatives, together with two reversible oxidation waves (0.94 and 1.27 V vs SCE in CH_2Cl_2), which are in consistence with the oxidation potentials of porphyrin derivatives. These data suggests that the porphyrin and perylene continue to behave as discrete units, indicating the linkage between the two moieties lacks a continuous delocalization pathway. This will be further confirmed by steady-state absorption spectra.

The **HOMO** and **LUMO** energies can be calculated with the redox potentials according to de Leeuw equation [27] and also listed in Table 1. Both **HOMO** and **LUMO** levels of porphyrin derivatives are higher than those of perylene derivatives, indicating a possible electron transfer from porphyrins to perylenes. This is in consistence with the literatures [12–20,28–30]. For the dyad **HTPP–PDI**, the **HOMO** locates on the porphyrin moiety while the **LUMO** locates on the perylene moiety, which is not overly surprising considering the orbital energies of the two moieties.

3.2. Steady-state absorption properties

The steady-state absorption spectra of the dyad along with **HTPPt, PDI**, and their 1:1 mixture (**HTPPt + PDI**) in dichloromethane are shown in Fig. 2. Compound **HTPPt** shows a 2 nm blue-shift of the absorption spectrum together with a little increase in the absorbance as comparing with compound **HTPP** due to the induction and steric effect of 4,6-dichloro-1,3,5-triazineamine group. This is in accordance with the increased **HOMO–LUMO** energy gap from **HTPP** (2.28 eV) to **HTPPt** (2.46 eV). So **HTPPt** was used to discuss the interaction between both units. The band at about 420 nm is the Soret band of the porphyrin moiety, which is an $a_{1u}(\pi)\rightarrow e_g(\pi^*)$ electron transition, assigned to the second excited state S_2 generated by $\pi\rightarrow\pi^*$ transition [31]. The Q-band of porphyrin moiety overlaps with the absorption band of perylene moiety in the region of 450–560 nm, leading to three absorption maxima at 460, 493 and 529 nm [32]. The weak absorption maxima at 594 nm and 651 nm are the rest of Q band of the porphyrin moiety

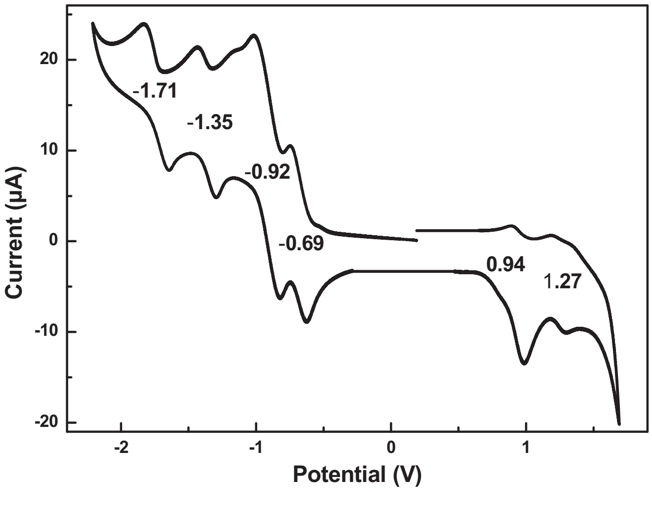

Fig. 1. Cyclic voltammetry curve of dyad **HTPP–PDI** in CH_2Cl_2 (vs SCE).

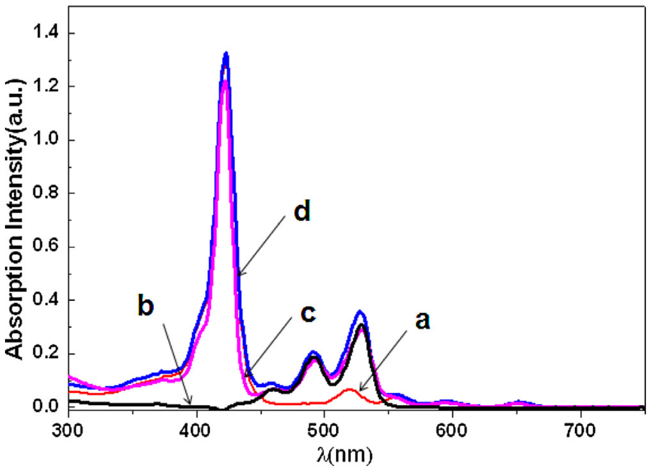

Fig. 2. Steady-state absorption spectra of **HTPPt** (a), **PDI** (b), **HTPP–PDI** (c) and 1:1 mixture of **HTPPt** and **PDI** (**HTPPt + PDI**) (d) in dichloromethane (5×10^{-6} mol/L).

[31]. The absorption spectrum of the dyad is identical with the sum of the spectra of **HTPPt** and **PDI** and greatly matches the solar spectrum. Same result was also obtained with the mixture. That is saying that, in the ground-state, the intermolecular nonbonding interaction and intramolecular through bonding interaction between both moieties are very weak so that we can ignore them. In another words, the porphyrin and perylene moieties in the dyad behave same as the discrete unites, in agreement with the electrochemical properties.

3.3. Steady-state fluorescence spectra

Fig. 3a shows the fluorescence emission spectra of the dyad, along with that of **HTPPt**, **PDI** and their 1:1 mixture (**HTPPt + PDI**) excited at 423 nm. **HTPPt** has a strong absorption at 423 nm while the absorption of **PDI** is very weak. Accordingly, the fluorescence of **HTPPt** is intense, which is almost the same as **HTPP** [21,22]. It is noted as two bands at 651 and 717 nm, which were also found in the spectrum of the dyad. But the fluorescence of the dyad was quenched by about 55% in comparison with that of **HTPPt** at same concentration, whereas little changes in the fluorescence intensity of the porphyrin moiety were showed in the mixture (**HTPPt + PDI**). These results indicate the possibility of intramolecular photoinduced energy and/or electron transfer from excited **HTPP** to **PDI** in the dyad, whereas the intermolecular interaction between both unites are so weak that it can be ignored. This is because of different distances, angles and relative orientations of two modules in two cases. Furthermore, two bands of weak fluorescence from **PDI** decrease either in the dyad or in the mixture, which can exclude the photoinduced energy transfer from excited porphyrin to perylene.

To explore the photophysical processes from the excited **PDI** to **HTPPt**, the fluorescence spectra at the excitation wavelength of 491 nm, where **PDI** has a strong absorption, were further determined. As shown in Fig. 3b, the emission spectrum of their mixture is almost the same as the sum of the spectra of both, except for a little reduction of the fluorescence from **PDI**. But in the dyad, the emission intensity from perylene moiety was quenched about 34% as compared to **PDI**. Concurrently the intensities at 651 and 717 nm were found to increase by about four times compared to **HTPPt**. Since the electron transfer from the perylene to the porphyrin is forbidden, the increased emissions from the porphyrin moiety of the dyad can be only explained by photoinduced through bonding energy transfer from the perylene to the porphyrin, which is accompanied with the decrease of emissions from perylene moiety. This is a Forster energy transfer indicated by the excitation spectrum of **HTPPt** at emission wavelength of 650 nm (see the insert of Fig. 3). Since the levels allowed, a hole transfer process from the **HOMO** of the perylene to that of the porphyrin cannot be ruled out completely.

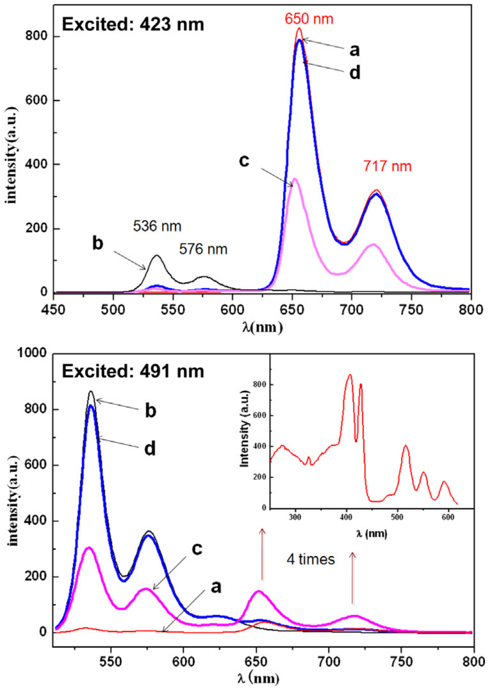

Fig. 3. Fluorescence emission spectra of **HTPPt** (a), **PDI** (b), **HTPP–PDI** (c) and 1:1 mixture of **HTPPt** and **PDI** (**HTPPt + PDI**) (d) in dichloromethane (5×10^{-6} mol/L). Excitation wavelength: 423 nm (top) and 491 nm (bottom). The insert is the fluorescence excitation spectrum of **HTPPt** at the emission wavelength of 650 nm.

3.4. Kinetic analysis

Fig. 4 provides the time-profiles for the decay of the perylene moiety at 541 nm and the porphyrin moiety at 651 nm in the dyad at

Table 2
Time-resolved fluorescence lifetimes τ (ns) of investigated compounds (5×10^{-6} mol/L).

Compound	Emission lifetime, (fraction %)			
	In dichloromethane		In toluene	
	PDI (λ_{em} = 541 nm)	HTPP (λ_{em} = 659 nm)	PDI (λ_{em} = 541 nm)	HTPP (λ_{em} = 659 nm)
HTPP	–	8.25		10.44
PDI	3.23	–	4.20	
HTPP + PDI	3.20	2.46 (6.9%) 8.25 (93.1%)	4.20	4.19 (6.0%) 10.36 (94.0%)
HTPP–PDI	0.64 (17.7%) 3.11 (82.3%)	1.52 (16.9%) 8.11 (83.1%)	1.87 (15.7%) 3.66 (84.8%)	2.85 (13.1%) 10.04 (86.9%)

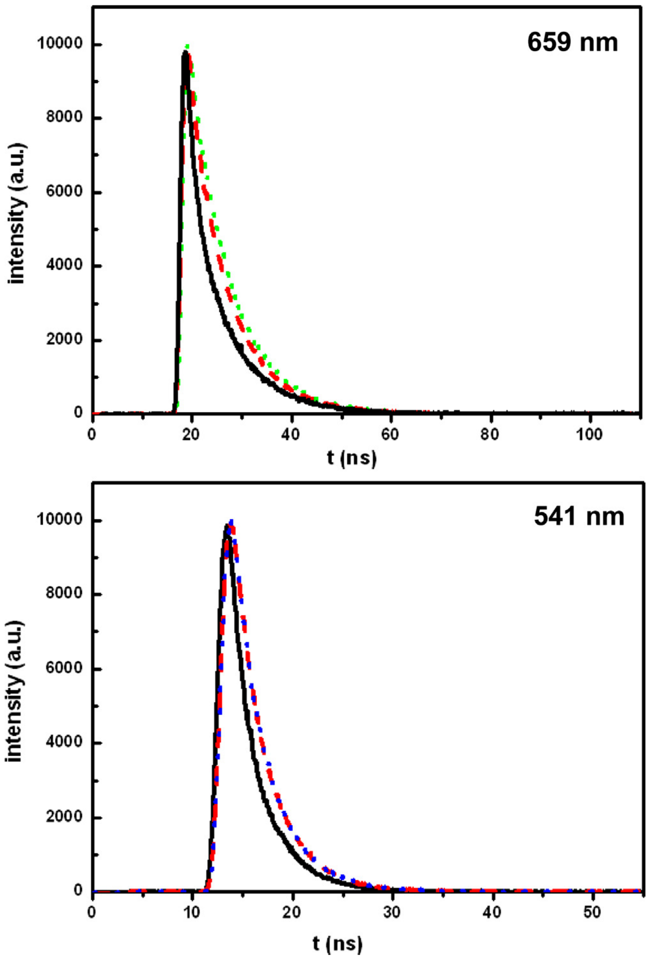

Fig. 4. Fluorescence decay profiles of **HTPPt** (green dot), **PDI** (blue dot), **HTPP–PDI** (solid) and 1:1 mixture of **HTPPt** and **PDI** (**HTPPt + PDI**) (dash) in dichloromethane (5×10^{-6} mol/L). Excitation wavelength: 459 nm; emission wavelength: 659 nm (top) and 541 nm (bottom). (For interpretation of the references to color in this figure legend, the reader is referred to the web version of the article.)

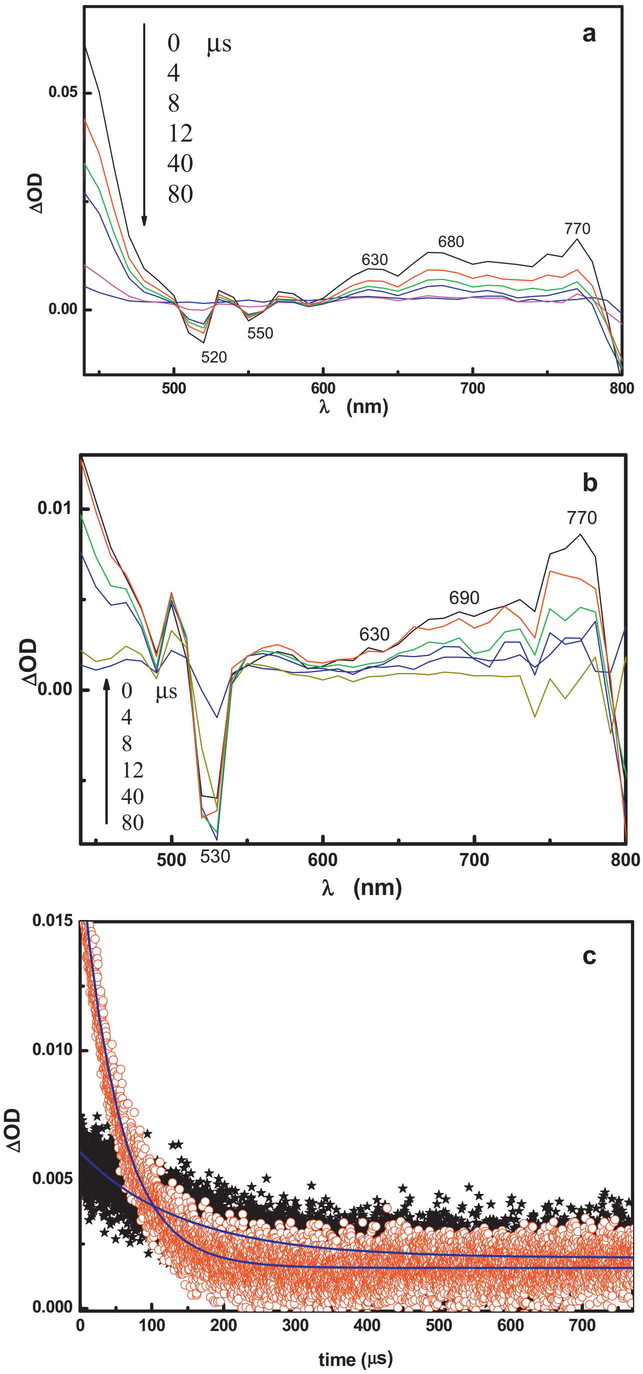

Fig. 5. Transient absorption spectra of **HTPP** (a) and **HTPP–PDI** (b) in dichloromethane (5×10^{-6} mol/L) at different times after flashing at 532 nm under nitrogen atmosphere. The (c) is the decay curves of **HTPP–PDI** at 440 (○) and 500 (⋆) nm together with blue fitting lines. (For interpretation of the references to color in this figure legend, the reader is referred to the web version of the article.)

an excitation wavelength of 459 nm. Both ^{1}**HTPPt*** and ^{1}**PDI*** follow monoexponential decay process with the calculated lifetimes of 8.01 and 3.22 ns, respectively (Table 2). These are consistent with the reports [33,34], showing that most ^{1}**HTPPt*** molecules undergo intersystem crossing to ^{3}**HTPPt*** and most ^{1}**PDI*** molecules relax by the solvation. In the 1:1 mixture (**HTPPt + PDI**), the presence of **HTPPt** does not change the decay process and emission lifetime of **PDI**, whereas the presence of **PDI** causes a two-order kinetic decay of the fluorescence from **HTPPt**. The minor fast component (6.9%) may be due to the weak intermolecular electron transfer according to previous discussions. Higher electron transfer rate intramolecularly than intermolecularly increases the fast component to 16.9% in the dyad, yielding the charge-separated excited state, **HTPP**$^{\bullet+}$–**PDI**$^{\bullet-}$. It is noted that the perylene fluorescence from the dyad also follows a biexponential decay equation with lifetimes of 0.64 and 3.11 ns. The fast process is attributed to the intramolecular photoinduced hole transfer from excited perylene to porphyrin and the slow one to the salvation relaxation of the excited perylenes. The shorter time constant (3.11 ns) than that of **PDI** (3.23 ns) confirms the Forster energy transfer from the excited perylene to the porphyrin. The results obtained with toluene solutions (Table 2) are similar, except that the lifetimes are longer in toluene than in dichloromethane.

Furthermore, the ^{1}**HTPP*** fluorescence decay process is comprised of two decay pathways. The first is the charge separation pathway with a lifetime of 1.52 ns and the second is the intersystem crossing pathway with a lifetime of 8.11 ns. It is worth mentioning that the fast charge separation pathway contributes only 16.9% of the entire decay. This smaller contribution from the faster decay pathway was also observed previously in other donor–acceptor systems [35–37]. The relative contribution from different competing decay pathways depends not only on the decay lifetime but also on the population leading to a specific decay pathway, which is determined by the factors such as the free energy change and

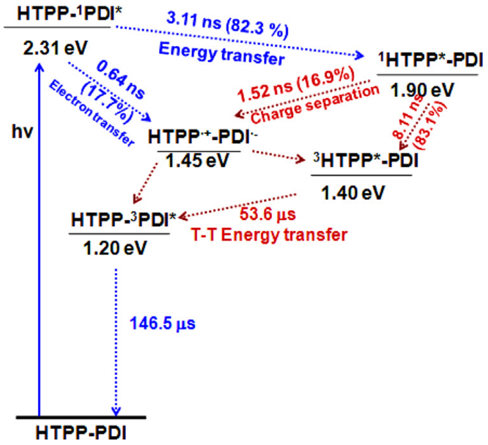

Fig. 6. Energy-level diagram and photophysical processes of dyad **HTPP–PDI**.

reorganization energy between the excited state and the relaxed state.

Fig. 5 gives the nanosecond transient absorption spectra and relative time-dependent decay profiles. The toluene solution was used because the dichloromethane solution turns quickly from red to green upon exposure to the laser pulse, indicating the destroy of the dyad by the radical cations (CH$_2$Cl$^{\bullet+}$) and carbocations (CH$_2$Cl^{+}) derived from the solvent [38]. The spectra in Fig. 5a show the features of pure ^{3}**HTPP*** and corresponding ground-state bleaching at 520, 550 and 590 nm because ^{1}**HTPP*** and stimulated emissions are no longer present after 4 µs upon irradiation based on the fluorescence decay spectra and literature [39]. In Fig. 5b, the feature in the range of 620–800 nm contains contributions of porphyrin radical cation **HTPP**$^{\bullet+}$, perylene radial anion **PDI**$^{\bullet-}$ and ^{3}**HTPP***. Since ^{3}**HTPP*** could not completely quenched by the oxygen experimentally, their absorptions overlap the absorptions of the charge-separated excited state, leading to a difficulty to analyze the lifetime of **PDI**$^{\bullet-}$ and **HTPP**$^{\bullet+}$.

Then the spectral changes of perylene transient species were investigated. The dyad exhibits typical absorption of triplet excited state (^{3}**PDI***) at about 500 nm [40], which is negligible in direct excitation via intersystem crossing of ^{1}**PDI*** [41], accompanied by a pronounced feature at 530 nm, which is attributed to the bleaching of perylene ground state (0,0) absorption [28]. The decay over time at 500 nm (Fig. 5c) appears to be monoexponential with a ^{3}**PDI*** lifetime of 146.5 µs. The absorption of the dyad at 440 nm, which follows a monoexponential decay kinetics with a lifetime of 53.6 µs (Fig. 5c) and can be quenched by the introduction of oxygen, is assigned to ^{3}**HTPP*** (52.6 µs for **HTPP** solution). The quantity of ^{3}**HTPP*** was found relative small in the dyad in comparison of the initial difference absorptions at 440 nm in Fig. 5a (0.0618) and b (0.0130).

An interesting phenomenon is showed in Fig. 5b that the absorptions of ^{3}**PDI*** at 500 nm and perylene ground state bleaching at 530 nm still rise at 4 µs after irradiation, which was found together with the reduced absorption in 600–800 nm. This increasing absorption of ^{3}**PDI*** at 4 µs is indicative of a triplet–triplet energy transfer from the porphyrin to the perylene moiety because all stimulated emissions from the dyad that might cause the bleaching of the perylene ground state have decayed out after 4 µs upon irradiation based on the fluorescence decay spectra.

The energy of charge-separated excited state, **HTPP**$^{\bullet+}$–**PDI**$^{\bullet-}$, is estimated by the offset of the **HOMO** level of **HTPP** (0.66 eV) and **LUMO** level of **PDI** (−0.79 eV). Perylene bisimide triplets have been reported to have an energy as low as 1.2 eV [42], much lower than the energy of the charge-separated excited state. Then the photophysical mechanism is schematized in the energy-level diagram of Fig. 6. Since the energy level of **HTPP**$^{\bullet+}$–**PDI**$^{\bullet-}$ is higher than those of triplet species, decay of **HTPP**$^{\bullet+}$–**PDI**$^{\bullet-}$ to ^{3}**PDI*** or ^{3}**PDI*** forms through spin inversion [19] is allowed.

4. Conclusions

In conclusion, the porphyrin–perylene dyad linked by a triazine group was successfully synthesized and showed an intramolecular photoinduced energy transfer from the perylene singlet to the porphyrin moiety, followed by an enhanced photo-induced electron transfer from the porphyrin singlet to the perylene moiety, thus resulting in the formation of the charge-separated state **HTPP**$^{\bullet+}$–**PDI**$^{\bullet-}$, which decays to the ground state via triplets. Though the lifetime of **HTPP**$^{\bullet+}$–**PDI**$^{\bullet-}$ may be relatively long, the photo-induced electron transfer is not efficient. In comparison to **HTPP**, the absorption of ^{3}**HTPP*** is very weak in dyad with a lifetime of 53.6 µs, close to that of **HTPP**. But the lifetime of ^{3}**PDI*** was found as long as about 146 µs, showing potential applications in the photodynamic therapy.

Acknowledgment

The authors would like to thank National Nature Sciences Foundation of China for the financial support (No. 20976122).

References

[1] G.F. Moore, G.W. Brudvig, Energy conversion in photosynthesis: a paradigm for solar fuel production, Annual Review of Condensed Matter Physics 2 (2011) 303–327.

[2] M.K. Panda, K. Ladomenou, A.G. Coutsolelos, Porphyrins in bio-spired transformations: light-harvesting to solar cell, Coordination Chemistry Reviews 256 (2012) 2601–2627.

[3] J. Ding, K. Feng, C.H. Tung, L.Z. Wu, Long-lived charge separation in a dyad system containing cyclometalated platinum(II) complex and ferrocene donor, Journal of Physical Chemistry C 115 (2011) 833–839.

[4] A.D. Quartarolo, S.G. Chiodo, N. Russo, A TDDFT investigation of bay substituted perylenediimides: absorption and intersystem crossing, Journal of Computational Chemistry 33 (2012) 1091–1100.

[5] A. Yella, H.W. Lee, H.N. Tsao, C. Yi, A.K. Chandiran, M.K. Nazeeruddin, E.W.G. Diau, S.M. Zakeeruddin, M. Grätzel, Porphyrin-sensitized solar cells with cobalt (II/III)-based redox electrolyte exceed 12 percent efficiency, Science 334 (2011) 629–634.

[6] S. Gupta, B.S. Dwarakanath, N.K. Chaudhury, A.K. Mishra, K. Muralidhar, V. Jain, In vitro and in vivo targeted delivery of photosensitizers to the tumor cells for enhanced photodynamic effects, Journal of Cancer Research Therapy 7 (2011) 314–324.

[7] R. Asano, A. Nagami, Y. Fukumoto, F. Yazama, H. Ito, I. Sakata, T. Akihiro, Synthesis and biological evaluation of new chlorine derivatives as potential photosensitizers for photodynamic therapy, Bioorganic and Medicinal Chemistry Letters 21 (2013) 2298–2304.

[8] Y.L. Wang, B. Cohen, L. Jicsinszky, A. Douhal, Femtosecond to second studies of a water-soluble porphyrin derivative in chemical and biological nanocavities, Langmuir 28 (2012) 4363–4372.

[9] L. Giribabu, P.S. Reeta, R.K. Kanaparthi, M. Srikanth, Y. Soujanya, Bis(porphyrin)–anthraquinone triads: synthesis, spectroscopy and photochemistry, Journal of Physical Chemistry A 117 (2013) 2944–2951.

[10] J.Y. Liu, M.E. El-Khouly, S. Fukuzumi, D.K. Ng, Mimicking photosynthetic antenna-reaction-center complexes with a (boron dipyrromethene)3–porphyrin–C60 pentad, Chemistry—A European Journal 17 (2011) 1605–1613.

[11] R. Agneeswari, V. Tamilavan, M. Song, J.W. Kang, S.H. Jin, M.H. Hyun, Synthesis of polymers containing 1,2,4-oxadiazole as an electron-acceptor moiety in their main chain and their solar cell applications, Journal of Polymer Science Part A: Polymer Chemistry 51 (2013) 2131–2141.

[12] S. Ikeda, N. Aratani, A. Osuka, A doubly 2,6-pyridylene-bridged porphyrin–perylene–porphyrin triad, Chemical Communications 48 (2012) 4317–4319.

[13] X.U. Yang, D. Zheng, R.R. Tang, X.H. Chen, Progress in the synthesis and application of porphyrin–perylene arrays, Chinese Journal of Organic Chemistry 29 (2009) 1906–1923.

[14] K. Tomizaki, R.S. Loewe, C. Kirmaier, J.K. Schwartz, J.L. Retsek, D.F. Bocian, D. Holten, J.S. Lindsey, Synthesis and photophysical properties of light-harvesting arrays comprised of a porphyrin bearing multiple perylene-monoimide accessory pigments, Journal of Organic Chemistry 67 (2002) 6519–6534.

[15] C. Jiao, N. Zu, K.W. Huang, P. Wang, J. Wu, Perylene anhydride fused porphyrins as near-infrared sensitizers for dye-sensitized solar cells, Organic Letters 13 (2011) 3652–3655.

[16] C. Jiao, K.W. Huang, C. Chi, J. Wu, Doubly and triply linked porphyrin–perylene monoimides as near IR dyes with large dipole moments and high photostability, Journal of Organic Chemistry 76 (2011) 661–664.

[17] S. Dong, X. Zhang, Y. Zhou, J. Jiang, Y. Bian, Perylene diimide-appended mixed (phthalocyaninato)(porphyrinato) europium(III) double-decker complex: synthesis, spectroscopy and electrochemical properties, Dyes and Pigments 91 (2011) 99–104.

[18] F. Wang, J. Tang, J. Liu, Y. Wang, R. Wang, L. Niu, L. Huang, Z. Huang, Highly efficient photoinduced electron transfer in a novel tetrakis(tetraphenylporphyrinatozinc)/perylenetetracarboxidiimidearray and its application to a photovoltaic device, Bulletin of the Chemical Society of Japan 84 (2011) 427–436.

[19] M. Ghirotti, C. Chiorboli, C.C. You, F. Würthner, F. Scandola, Photoinduced energy and electron-transfer processes in porphyrin–perylene bisimide symmetric triads, Journal of Physical Chemistry A 112 (2008) 3376–3385.

[20] M.R. Wasielewski, Self-assembly strategies for integrating light harvesting and charge separation in artificial, Accounts of Chemical Research 42 (2009) 1910–1921.

[21] M. Tao, L. Liu, D. Liu, X. Zhou, Photoinduced energy and electron transfer in porphyrin–anthraquinone dyads bridged with a triazine group, Dyes and Pigments 85 (2010) 21–26.

[22] M. Tao, D. Liu, M. Zhang, X. Zhou, Photoinduced energy and electron transfer in porphyrin–oxadiazole dyads, Acta Chimica Sinica 66 (2008) 1252–1258.

[23] R. Luguya, L. Jaquinod, F.R. Fronczek, Synthesis and reactions of meso-(p-nitrophenyl)porphyrins, Tetrahedron 60 (2004) 2757–2763.

[24] M.W. Holman, R. Liu, D.M. Adams, Single-molecule spectroscopy of interfacial electron transfer, Journal of American Chemistry Society 125 (2003) 12649–12654.

[25] C.C. You, R. Dobrawa, C.R. Saha-Moller, F. Wurthner, Metallosupramolecular dye assemblies, Topics in Current Chemistry 258 (2005) 39–82.

[26] J.P. Gisselbrecht, M. Gross, E. Vogel, P. Scholz, M. Broring, J.L. Sessler, Redox properties of hemiporphycene and isoporphycene – comparison with those of porphyrin and other porphyrin isomers, porphycene and corrphycene, Journal of Electroanalytical Chemistry 507 (2001) 244–249.

[27] D.M. de Leeuw, M.M.J. Simenon, A.R. Brown, R.E.F. Einerhand, Stability of n-type doped conducting polymers and consequences for polymeric microelectronic devices, Synthetic Metals 87 (1997) 53–59.

[28] C. Kirmaier, H. Song, E. Yang, J.K. Schwartz, E. Hindin, J.R. Diers, R.S. Loewe, K. Tomizaki, F. Chevalier, L. Ramos, R.R. Birge, J.S. Lindsey, D.F. Bocian, D. Holten, Excited-state photodynamics of perylene- porphyrin dyads. 5. Tuning light-harvesting characteristics via perylene substituents. Connection motif, and three-dimensional architecture, Journal of Physical Chemistry B 114 (2010) 14249–14264.

[29] M.T. Indelli, C. Chiorboli, F. Scandola, E. Iengo, P. Osswald, F. Wurthner, Photoinudced processes in self-assembled porphyrin/perylene bisimide metallosupromolecular boxes, Journal of Physical Chemistry B 114 (2010) 14495–14504.

[30] S.M. Mickley Conron, L.E. Shoer, A. Smeigh, A.B. Ricks, M.R. Wasielewski, Photoinitiated electron transfer in zinc porphyrin–perylenediimide cruciforms and their self-assembled oligomers, Journal of Physical Chemistry B 117 (2013) 2195–2204.

[31] R.F. Kelley, W.S. Shin, B. Rybtchinski, L.E. Sinks, M.R. Wasielewski, Photoinitiated charge transport in supramolecular assemblies of a 1,7,N,N′-tetrakis(zincporphyrin)-perylene-3,4:9,10-bis(dicarboximide), Journal of American Chemistry Society 129 (2007) 3173–3181.

[32] M.J. Ahrens, R.F. Kelley, Z.E.X. Dance, M.R. Wasielewski, Photoinduced charge separation in self-assembled cofacial pentamers of zinc-5,10,15,20-tetrakis(perylenediimide)porphyrin, Physical Chemistry Chemical Physics 9 (2007) 1469–1478.

[33] J.E. Haley, W. Su, K.M. Singh, J.L. Monahan, J.E. Slagle, D.G. McLean, T.M. Cooper, Effect of b-bromo substitution on the photophysical properties of meso-phenyl, meso-carbazole, and meso-triphenylamine porphyrins, Journal of Porphyrins and Phthalocyanines 16 (2012) 370–379.

[34] M.T. Vagnini, A.L. Smeigh, J.D. Blakemore, S.W. Eaton, N.D. Schley, F. D'Souza, R.H. Crabtree, G.W. Brudvig, D.T. Co, M.R. Wasielewski, Ultrafast photodriven intramolecular electron transfer from an iridium-based water-oxidation catalyst to perylene diimide derivatives, Proceedings of the National Academy of Sciences of the United States of America 109 (2012) 15651–15656.

[35] V.L. Gunderson, E. Krieg, M.T. Vagnini, M.A. Iron, B. Rybtchinski, M.R. Wasielewski, Photoinduced singlet charge transfer in a ruthenium(II) perylene-3,4:9,10-bis(dicarboximide) complex, Journal of Physical Chemistry B 115 (2011) 7533–7540.

[36] S. Xiao, M.E. El-Khouly, Y. Li, Z. Gan, H. Liu, L. Jiang, Y. Araki, O. Ito, D. Zhu, Dyads and triads containing perylenetetracarboxylic diimide and porphyrin: efficient photoinduced electron transfer elicited via both excited singlet states, Journal of Physical Chemistry B 109 (2005) 3658–3667.

[37] Z.Q. Yan, B. Xu, Y.J. Dong, W.J. Tian, A.W. Li, The photophysical properties and two-photon absorption of novel triphenylamine-based dendrimers, Dyes and Pigments 90 (2011) 269–274.

[38] W.E. Ford, H. Hiratsuka, P.V. Kamat, Photochemistry of 3,4,9,10-perylenetetracarboxylic dianhydride dyes. 4. Spectroscopic and redox properties of oxidized and reduced forms of the bis(2,5-di-tert-butylphenyl)imide derivative, Journal of Physical Chemistry 93 (1989) 6692–6696.

[39] S.I. Yang, R.K. Lammi, S. Prathapan, M.A. Miller, J. Seth, J.R. Diers, D.F. Bocian, J.S. Lindsey, D. Holten, Synthesis and excited-state photodynamics of perylene-porphyrin dyads. Part 3. Effects of perylene, linker, and connectivity on ultrafast energy transfer, Journal of Materials Chemistry 11 (2001) 2420–2430.

[40] C. Huang, S. Barlow, S.R. Marder, Perylene-3,4,9,10-tetracarboxylic acid diimides: synthesis, physical properties, and use in organic electronics, Journal of Organic Chemistry 76 (2011) 2386–2407.

[41] S. Suzuki, M. Kozaki, K. Nozaki, K. Okada, Recent progress in controlling photophysical processes of donor–acceptor arrays involving perylene diimides and boron-dipyrromethenes, Journal of Photochemistry and Photobiology C: Photochemistry Review 12 (2011) 269–292.

[42] W.E. Ford, P.V. Kamat, Photochemistry of 3,4,9,10-perylenetetracarboxylic dianhydride dyes. 3. Singlet and triplet excited-state properties of the bis(2,5-di-tert-butylphenyl)imide derivative, Journal of Physical Chemistry 91 (1987) 6373–6380.